



A Journal of the Gesellschaft Deutscher Chemiker

Angewandte Chemie

GDCh

International Edition

www.angewandte.org

Accepted Article

Title: Selective Catalytic Dehydrogenative Oxidation of Bio-polyols to Lactic Acid

Authors: Jiajie Wu, Lingyun Shen, Sai Duan, Zhe-Ning Chen, Qingshu Zheng, Yaoqi Liu, Zheming Sun, James H. Clark, Xin Xu, and Tao Tu

This manuscript has been accepted after peer review and appears as an Accepted Article online prior to editing, proofing, and formal publication of the final Version of Record (VoR). This work is currently citable by using the Digital Object Identifier (DOI) given below. The VoR will be published online in Early View as soon as possible and may be different to this Accepted Article as a result of editing. Readers should obtain the VoR from the journal website shown below when it is published to ensure accuracy of information. The authors are responsible for the content of this Accepted Article.

To be cited as: *Angew. Chem. Int. Ed.* 10.1002/anie.202004174

Link to VoR: <https://doi.org/10.1002/anie.202004174>

Selective Catalytic Dehydrogenative Oxidation of Bio-polyols to Lactic Acid

Jiajie Wu,^[a] Lingyun Shen,^[a] Sai Duan,^[b] Zhe-Ning Chen,^[b] Qingshu Zheng,^[a] Yaoqi Liu,^[a] Zheming Sun,^[a] James H. Clark,^[c] Xin Xu,^{*[b]} and Tao Tu^{*[a,d,e]}

Dedicated to Prof. Dr. Karl Heinz Dötz.

- [a] J. Wu, L. Shen, Dr. Q. Zheng, Y. Liu, Dr. Z. Sun, and Prof. Dr. T. Tu
Shanghai Key Laboratory of Molecular Catalysis and Innovative Materials, Department of Chemistry
Fudan University
2005 Songhu Road, Shanghai 200438 (China)
E-mail: taotu@fudan.edu.cn
- [b] S. Duan, Dr. Z.-N. Chen, Prof. Dr. X. Xu
Collaborative Innovation Center of Chemistry for Energy Materials, MOE Laboratory for Computational Physical Science
Fudan University
2005 Songhu Road, Shanghai 200438 (China)
E-mail: xxchem@fudan.edu.cn
- [c] Prof. J. H. Clark
Green Chemistry Centre of Excellence
University of York
York YO105DD, UK
- [d] Prof. Dr. T. Tu
State Key Laboratory of Organometallic Chemistry
Shanghai Institute of Organic Chemistry, Chinese Academy of Sciences
354 Fenglin Road, Shanghai 200032 (China)
- [e] Prof. Dr. T. Tu
College of Chemistry and Molecular Engineering
Zhengzhou University
100 Kexue Avenue, Zhengzhou 450001 (China)

Supporting information for this article is given via a link at the end of the document.

Abstract: The global demand for lactic acid (LA) is increasing due to its prominence as a bio-based platform molecule and its successful application as a monomer for bio-plastics manufacture. The development of new, selective, and sustainable approaches for LA synthesis using highly active catalysts is becoming critically important. Although N-heterocyclic carbene (NHC) iridium complexes have been proven as promising molecular catalysts for this purpose, their instabilities have seriously hindered their potential utilization especially in commercial applications. Here, we report for the first time that a porous self-supported NHC-iridium coordination polymer can efficiently prevent the clusterization of corresponding NHC-Ir molecules and can function as a solid molecular recyclable catalyst for dehydrogenation of a number of bio-polyols to make LA with excellent activity (97%) and selectivity (>99%), and up to 5700 turnover number could be achieved in a single batch, due to the synergistic participation of the Ba²⁺ and hydroxide ions, as well as the blockage of unwanted pathways by adding methanol. Our findings demonstrate a potential route for the industrial production of LA from cheap and abundant bio-polyols, including sorbitol.

Introduction

With the goal of alleviating our serious dependence on fossil fuels, the catalytic conversion of inexpensive bio-renewables into fuels and value-added chemicals has received considerable attention during the last decade.^[1] Bio-polyols such as sorbitol, glycerol, xylitol, and mannitol have been regarded as among the most

promising renewable carbon sources for this purpose, as all of them are readily accessed by simple hydrolysis of agricultural residues, lignin, cellulose, and hemicellulose.^[2] An emerging technique for their utilization is the direct conversion of bio-polyols such as sorbitol, using multifunctional catalysts.^[2] Apart from its applications in food, cosmetics, and paper industries as additives,^[3] sorbitol is also a platform molecule useful for the synthesis of various valuable fine chemicals, including ethylene glycol (EGO),^[4] 1,2-propanediol,^[4b] and lactic acid (LA).^[5] Given the steady increase in the price and annual consumption of LA over the last ca. 20 years, largely as a result of the increasing global demands for biodegradable polylactide,^[6] there is a particular merit in developing efficient and selective approaches for LA production from sorbitol and other bio-polyols.

Although a great deal of effort has been devoted to this important transformation, only two strategies, i.e., hydrogenolysis and dehydrogenative oxidation, have been realized so far.^[4a,5] But in both cases, the yield and the selectivity of LA were quite low and well below the industrial requirement even at elevated pressures and temperatures. As shown in Figure 1a, the best result for this challenging transformation is a yield of 40% with a selectivity of 82% to LA. This was based on bis-N-heterocyclic carbene (NHC) iridium complex **1**,^[7] which is easily converted to various inactive species (like **2** in Figure 1a, a dimer with Ir-Ir bond) due to the possible clusterization (dimerization,^[5] trimerization, tetramerization, and even multimerization)^[8] of NHC-Ir complexes, could not be avoided by simply increasing the bulkiness of the NHC ligands.^[5] Despite the low performance, this is still a very attractive protocol because clean energy H₂ as well

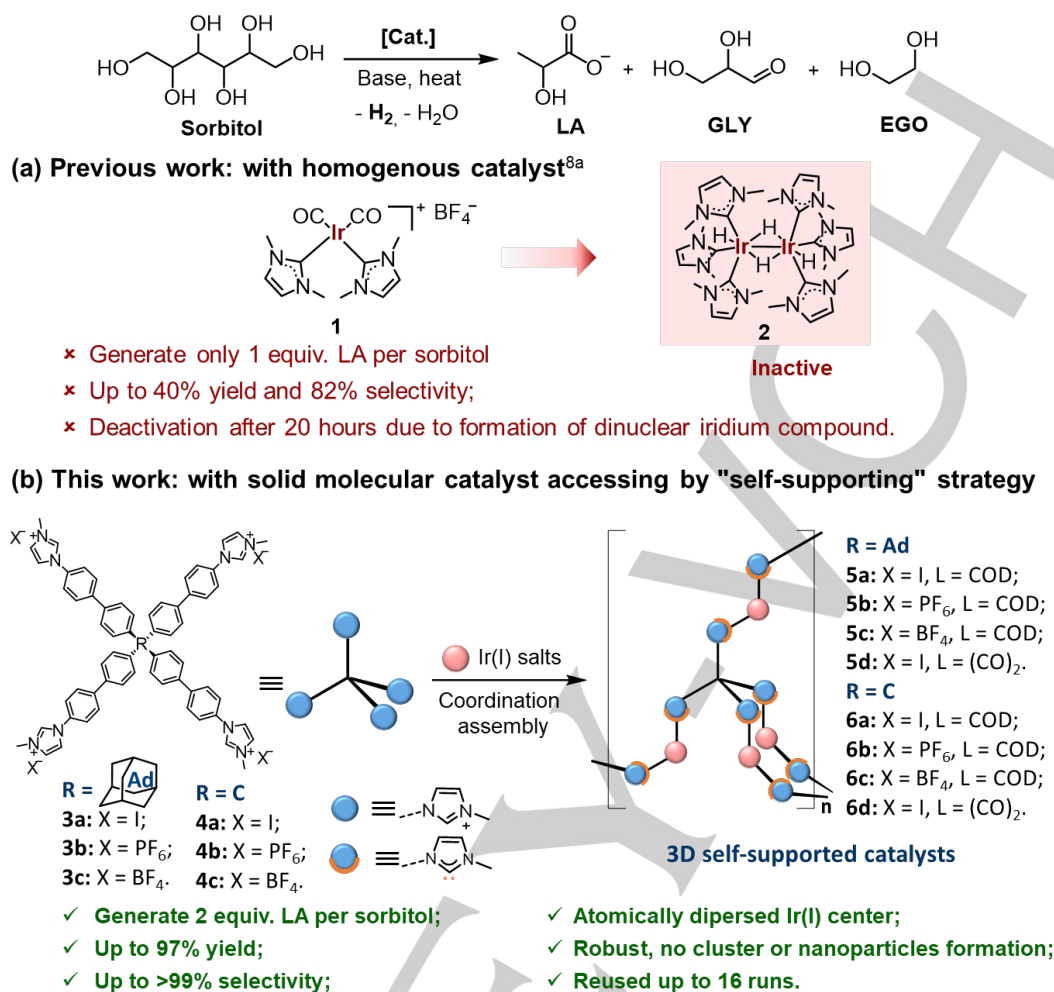


Figure 1. Oxidative dehydrogenation of sorbitol to LA. a) Previous work: Catalyzed by homogenous catalyst NHC-Ir **1** (yield was calculated based on 1 equiv. LA formed per sorbitol according to Ref 8a). b) This work: Catalyzed by self-supported catalysts **5-6** prepared by coordination assembly (yield was calculated based on 2 equiv. LA formed per sorbitol).

as LA was produced.^[9] Presumably, the prevention of multi-nuclear iridium clustering may provide a viable way to resolve the problems and move this bio-resource conversion towards commercial viability.

Recently, the "self-supporting" approach has emerged as a new and efficient strategy for catalyst immobilization using coordination assembly of the corresponding ligands with metal ions.^[10] The resulting self-supported catalysts can function as solid molecular catalysts and can even exhibit a higher catalytic activity than the corresponding homogenous catalysts as found in several cases.^[11] In our experience, the "self-supporting" strategy looks promising for our purpose here, as the ditopic ligands can isolate the catalytically active metal ions and block the possible clusterization of the iridium catalysts.^[5,8] Therefore, in the present work, we have synthesized a series of three-dimensional (3D) porous NHC-Ir coordination polymeric assemblies (**5a-d** and **6a-d**) by using the "self-supporting" strategy (Figure 1b). These coordination assemblies efficiently hamper the possible clusterization of iridium species, and function as solid molecular catalysts with excellent catalytic activity and selectivity for LA

production from sorbitol. Furthermore, the reaction mechanisms have been disclosed at the state-of-the-art first-principles level. It is also noteworthy that one molecule of sorbitol generates two molecules of LA in this protocol rather than that one sorbitol produced only one LA in the previous study.^[5] The present protocol is thus obviously more atom economic. These significant advances have greatly increased the industrial potential for this important transformation.

Results and Discussion

Syntheses and characterizations of the three-dimensional NHC-Ir coordination assemblies. With the "self-supporting" strategy in mind, tetraimidazolium iodides **3** and **4** with two different rigid cores adamantane (Ad) or carbon (C) were synthesized via Suzuki coupling and N-methylation reactions (see Supporting Information (SI) for more details). The diphenyl fragment was introduced to ensure that after deprotonation with a

base, the resultant tetradentate terminal NHCs were geometrically well-separated from each other and could only further bind to different Ir centers to generate an extended 3D supramolecular structure via the coordination assembly (Figure 1b). Subsequently, tetraimidazolium salts with different ions were prepared by treating the iodides **3a** and **4a** with NH_4PF_6 or Et_3OBF_4 to produce salts **3b-c** and **4b-c**, respectively. After deprotonation by lithium bis(trimethylsilyl)amide (LiHMDS) and further coordination with the selected iridium precursors ($[\text{Ir}(\text{acac})(\text{CO})_2]$, acac = acetylacetonato or $[\text{Ir}(\text{COD})\text{Cl}]_2$, COD = 1,5-cyclooctadiene), a number of 3D coordination assemblies **5a-d** and **6a-d** containing different counter-ions (I^- , BF_4^- or PF_6^-) and ancillary ligands (CO or COD) were readily obtained in excellent yields (95-99%). For comparison, one dimensional (1D) linear NHC-Ir coordination assemblies **7a-b** were also synthesized from the corresponding bis-imidazolium salts based on our previous reports.^[11]

All obtained coordination assemblies **5a-d**, **6a-d** and **7a-b** are essentially insoluble in water and all organic solvents tested. Thus, their compositions can only be fully characterized by using solid-state analytical techniques. The morphologies of the freshly prepared 3D coordination assemblies **5a-d** and **6a-d** were investigated by scanning electron microscopy (SEM). Similar to the 1D NHC-Ir assemblies **7a-b**,^[11] the 3D NHC-Ir assemblies **5a-d** and **6a-d** are composed of some irregular nano-particles (Figure 2a, and Figures S2-S10). The transmission electron microscopy (TEM) confirmed this observation (Figure 2b and Figures S11-13). The average size for NHC-Ir assembly **5a** is ca. 450 nm as measured by dynamic light scattering (DLS, Figure S35), which is slightly larger than the diameter observed by SEM (around ca. 300 nm, Figure 2a). This difference might be caused by a solvent effect in the hydrated state.^[12]

Furthermore, taking solid **5a** as an example, the amorphous nature of NHC-Ir coordination assemblies was shown by the powder X-ray diffraction (PXRD) patterns (Figure S18). For comparison, a homogeneous NHC-Ir complex **8** was synthesized from 1-methyl-3-phenylimidazolium iodide and $[\text{Ir}(\text{COD})\text{Cl}]_2$, and was fully characterized by ^1H and ^{13}C NMR spectra (Figures S61-62), and high resolution mass spectrometry (see SI for details). Pleasingly, most peaks in the solid ^{13}C NMR spectra of assembly **5a** are clearly assignable to the structural carbon atoms (Figure S63). The peak at 174.4 ppm is attributed to the C_{NHC} of solid **5a**, and the corresponding signal in the spectra of the molecular complex **8** is at 175.8 ppm. X-ray photoelectron spectroscopy (XPS) signals of the agglomerated iridium nano-particles were not observed in solid **5a** (Figure S20). Instead, only Ir(I) signals at 62.2 ($4f_{5/2}$) eV and 65.2 ($4f_{7/2}$) eV that correspond to the two characteristic bands of molecular iridium species emerge for both solid **5a** and complex **8** (Figure S29). Energy dispersive X-ray spectroscopy (EDX) quantification of **5a** revealed a uniform distribution of all expected elements, including C, Ir and, N, in the assembly matrix (Figure 2c). Furthermore, magnified high-angle annular dark-field scanning transmission electron microscopy (HAADF-STEM) images showed well dispersed white dots, indicating that individual Ir atoms are atomically dispersed in the

matrix of solid **5a** (Figure 1d). All these data clearly indicated that the coordination environment of the Ir center in the solid **5a** is quite similar to that in the molecular complex **8**. Thus assemblies such as solid **5a** can be expected to function as molecular catalysts.

To measure the porosity of the NHC-Ir coordination assemblies, N_2 adsorption/desorption studies were carried out (Figure S34). The 3D coordination assembly **5a** has a surface area of $388 \text{ m}^2\text{g}^{-1}$ that is almost 50 times greater than that of 1D coordination assembly **7a** ($8 \text{ m}^2\text{g}^{-1}$), highlighting the porous structure of the solid assembly **5a**.

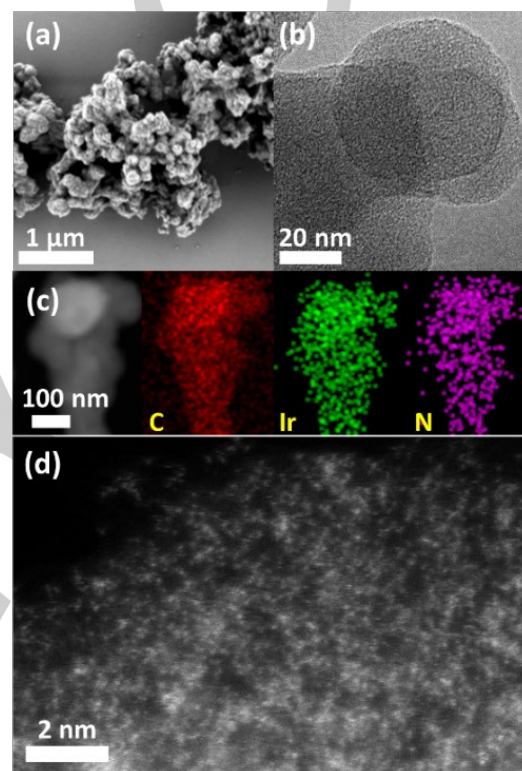


Figure 2. Morphology studies of catalyst **5a**. a) SEM image of **5a**. b) TEM image of **5a**. c) EDS mapping of **5a**. d) Magnified HAADF-STEM image of **5a**, white dots represent individual Ir atoms, indicating that the iridium centers are atomically dispersed in the assembly matrix.

The catalytic activity of the NHC-Ir coordination assemblies.

The catalytic activities of the characterized NHC-Ir coordination assemblies were then tested for the oxidative dehydrogenation of bio-polyols initially using D-sorbitol as the substrate. In the presence of 0.2 mol % NHC-Ir coordination assemblies, 3 mmol D-sorbitol and 1.5 equiv. of $\text{Ba}(\text{OH})_2$ were heated in a sealed tube at 160°C for 6 hours.^[2a] Compared to the molecular NHC-Ir complex **1**, linear 1D NHC-Ir coordination assembly **7b** showed a slight improvement in the yield and selectivity to LA (48% vs 35% for **7b** and **1**, respectively, Figure 3a). These observations are important because: (i) a supported catalyst normally results in a worse yield and selectivity than the corresponding homogenous privileged catalysts;^[13] (ii) an extended reaction time or increased

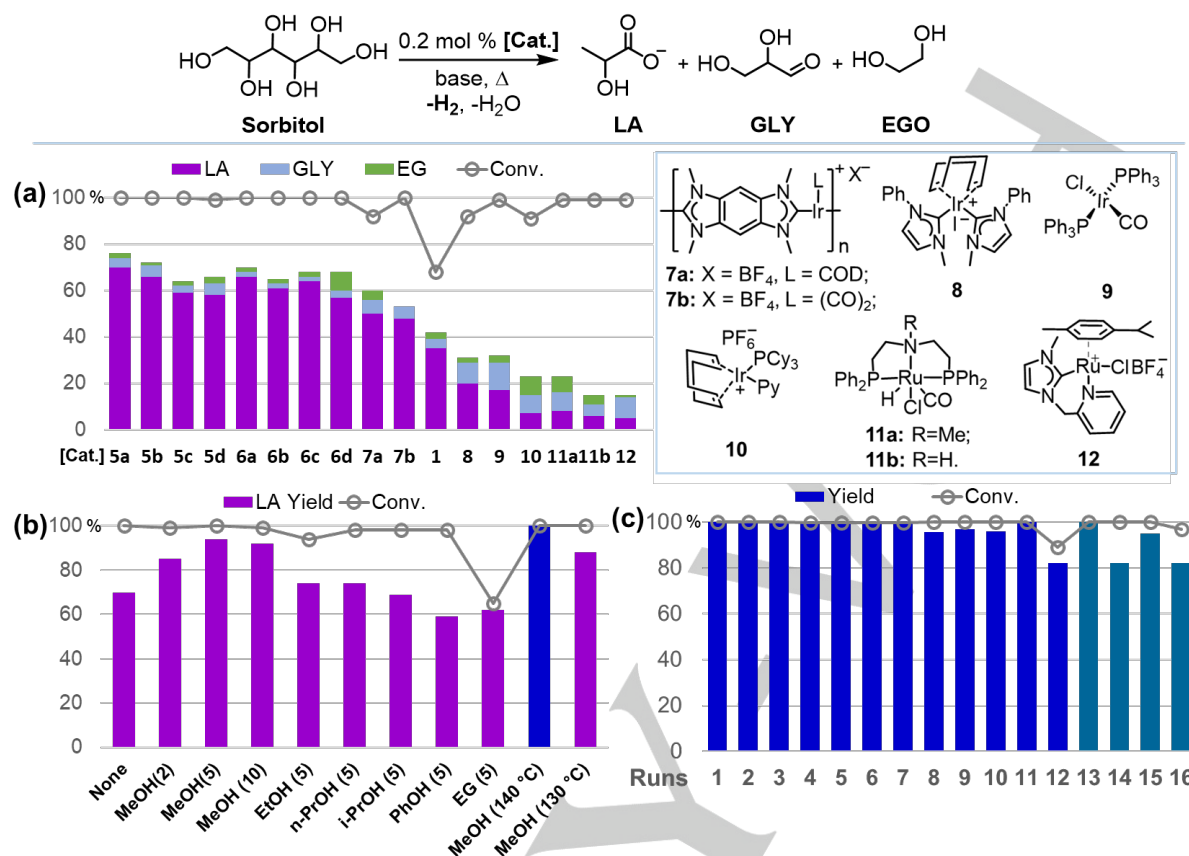


Figure 3. Optimization of reaction conditions and reusability of the catalyst for oxidative dehydrogenation of sorbitol to LA. a) Catalyst screening with 1.5 equiv. $\text{Ba}(\text{OH})_2$, 3 mmol D-sorbitol, 0.2 mol % catalyst, in 0.3 mL H_2O at 160 °C for 6 hours. b) Influence of alcohol additives and temperatures. Reactions were carried out with 3 mmol D-sorbitol, 0.2 mol% **5a**, 2.5 equiv. $\text{Ba}(\text{OH})_2 \cdot 8\text{H}_2\text{O}$, and 0–10 equiv. of selected alcohols as additional additives at 150 °C (left 9 purple bars); 5 equiv. MeOH at 140 °C (blue bar) and at 130 °C (right purple bar) for 12 hours. c) Reusability of catalyst **5a**. Reactions were carried out with 3 mmol D-sorbitol, 0.2 mol% **5a** and 2.5 equiv. $\text{Ba}(\text{OH})_2 \cdot 8\text{H}_2\text{O}$ at 140 °C for 12 hours (1–12 runs, the blue bars), or with extended reaction time to 24 hours (after the 12th run, the turquoise bars). All the conversions, yields and selectivities were determined by an HPLC analysis and calculated based on 2 equiv. LA formed per sorbitol.

temperature will not improve the product yields due to deactivation of the molecular catalysts through clusterization.^[5,8] Furthermore, when other iridium and ruthenium complexes **8–12**, privileged molecular catalysts in various dehydrogenative transformations,^[8a,14] were applied to this reaction, inferior yields and selectivities were observed (Figure 3a). Therefore, the “self-supporting” strategy can indeed be considered as an effective approach to increase the yield and selectivity for the dehydrogenative transformation of sorbitol to LA.

As porous catalysts can accelerate mass and heat transfer^[15] and thus facilitate reactions, we then tested the porous 3D NHC-Ir coordination assemblies **5a–d** and **6a–d** (See Figure 3a). Compared to the 1D assembly **7**, the 3D assemblies **5** and **6** exhibited slightly higher yields and selectivities (57%–70% vs 48%–50%, Figure 3a), suggesting that a high porosity of the catalysts was beneficial to the synthesis of LA. Higher selectivities were obtained by using the assemblies **5a–d** with a tetrakisphenyladamantane core ($\text{R} = \text{Ad}$, Figure 3a). This may indicate that the substrate can contact the catalytic sites better for a catalyst that has a higher surface area and a larger pore size.

Catalyst composition has a significant effect on the reaction, and the bidentate COD ligand was found to be better than the monodentate CO ligand in both cases (See **5a** vs **5b** and **6a** vs **6b** in Figure 3a). In contrast with non-coordinating BF_4^- and PF_6^- anions, the iodide anion may well be located close to the iridium center, leading to enhanced activity and selectivity (See **5a** vs **5c–d** and **6a** vs **6c–d** in Figure 3a). With all these outcomes, solid assemblies **5a** has been identified as the most efficient catalyst for the oxidative dehydrogenation of sorbitol with a yield of 70% for LA within 6 hours.

The other reaction parameters, including base, additives, and reaction temperature, were then investigated (See Table S1 and Figure S1). We found that bases played a critical role in the transformation. Weak bases, such as K_3PO_4 and K_2CO_3 , all resulted in only traces of LA (See entries 2 and 3 in Table S1). A strong base, e.g., $t\text{-BuOK}$, was also unable to convert sorbitol. We found that the presence of the hydroxide ion OH^- is essential to the dehydrogenation process (See entry 4 in Table S1). Therefore, other alkali hydroxides (i.e., NaOH and CsOH) and some alkaline-earth metal hydroxides (e.g. $\text{Ca}(\text{OH})_2$ and $\text{Ba}(\text{OH})_2$) were tested

under otherwise identical reaction conditions. The use of $\text{Ca}(\text{OH})_2$ led to equal selectivity between LA and EGO. However, in contrast to other metal hydroxides, up to 90% conversion of sorbitol was achieved using $\text{Ba}(\text{OH})_2$, with an LA selectivity up to 53%. On the other hand, little reaction occurred when BaCO_3 or BaCl_2 was used (See entries 14 and 15 in Table S1). The quantity of $\text{Ba}(\text{OH})_2$ and the reaction temperature were also found to be important parameters in the reaction. Up to 98% conversion of sorbitol with up to 70% yield of LA was observed using 2.5 equiv. $\text{Ba}(\text{OH})_2$ at 150 °C (See entries 11 to 13 in Table S1).

Mechanistic studies. We carried out a time-dependent study on the oxidative dehydrogenation of sorbitol using 0.2 mol % solid catalyst **5a** in order to better understand the possible reaction pathways. The liquid products in the reaction mixtures, ranging from the unreacted sorbitol and the products LA, glyceraldehyde (GLY), EGO, methanol and ethanol, etc., were analyzed directly by High Performance Liquid Chromatography (HPLC) with a refractive index (RI) detector. The concentration profiles were plotted as a function of time in Figure S72. As expected, under alkaline conditions and with hydrogen liberation, no sugar product was observed. The reaction rate was found to strongly depend on sorbitol concentration: after 1 hour over 60% of sorbitol was consumed, a 90% conversion was reached after 5 hours. Interestingly, the LA selectivity stayed ca. 70% during the reaction, while EGO increased almost linearly during the first 30 minutes and then decreased slowly, indicating that EGO may be one of the reaction intermediates. By extending the reaction time, short aliphatic alcohols (MeOH and EtOH) were generated, possibly formed by further cleavage of $\text{LA}^{[5]}$ and hydrogenation of EGO along with the liberation of hydrogen.

The first step in the sorbitol transformation is an iridium-catalyzed dehydrogenation step leading to glucose or fructose generation. Here complex **8** was used as a molecular model of the catalytic center of the NHC-Ir coordination assemblies (Figure 4a). Our density functional theory (DFT) calculations^[16] demonstrated that the NHC-Ir-catalyzed dehydrogenative reaction here is actually a redox-neutral process (i.e., from an Ir(I) species to an Ir(I) species without any valence change). As shown in Figure 4a, partial dissociation of the COD ligand from η^2 to η^1 is the initial step to generate the active catalytic Ir(I) species **A**. Subsequently, with the participation of the base, a) glucose and b) fructose are generated with the activation free energies of 25.2 and 26.5 kcal/mol (TS1 and TS2), respectively. The primary (α) and the secondary (β) hydroxyl groups in sorbitol provide the proton to the base, and concertedly H-bond to the C_α or the C_β site of sorbitol,^[17] forming an iridium hydride intermediate **B**. When the COD ligand bis-chelates to the Ir(I) center (from η^1 to η^2), a penta-coordinated hydride intermediate **C** is then formed. After hydrogen liberation, the initial NHC-Ir catalyst **8** is regenerated. As shown in Figure 4a, although the generation of glucose seems slightly more favorable than that of fructose (TS1 vs. TS2), their activation free energies for the catalyst regeneration are very similar (TS3: 35.5 vs. 35.9 kcal/mol), diminishing the energy difference for these two possible reaction pathways. This similarity in kinetics is also supported by the calculated

thermodynamics (A comparison with other possible catalytic species is shown in the SI, Schemes S6 - S8). In addition, it is worth noting that, according to the DFT calculations, the NHC ligands of the catalysts are firmly bonded to the Ir(I) center. The dissociation free energy of the NHC ligand from the Ir(I) center is 23.6 kcal/mol. On the other hand, the conversion from η^2 to η^1 for the COD ligand is more feasible (19.5 kcal/mol), which further confirms the structural stability of the solid catalyst **5a**.

The second step of the transformation involves the retro-aldol reaction of glucose and fructose, forming smaller carbohydrate molecules including glycolaldehyde plus erythrose (via the [2+4] route for the former, Figure 4b) or dihydroxyacetone plus glyceraldehyde (via the [3+3] route for the latter, Figure 4c). The reaction mechanisms for the conversion of these two C3 molecules to LA are well established.^[16] It is also known that the C4 molecule (i.e., erythrose) can be further converted into lactate and methanol^[5] (Figure 4b,c). DFT calculations give a barrier of 46.8 kcal/mol for the [2+4] route via TS4 and 45.0 kcal/mol for the [3+3] route via TS5, showing that the direct C-C cleavage via these two routes are not really feasible. With the participation of Ba^{2+} /hydroxide, the corresponding barriers are dramatically reduced to 22.6 and 20.2 kcal/mol via TS4Ba and TS5Ba, respectively, demonstrating undoubtedly the key role played by the Ba^{2+} ion and the base (Figs. 4b and c). Considering that the participation of Ba^{2+} /hydroxide can facilitate the generation of lactate species both kinetically and thermodynamically, a high activity and a high selectivity towards lactate in our experiments has thus been confirmed.

These proposed reaction mechanisms involve several reversible reactions, e.g., the retro-aldol reaction, and the isomerization between glucose and fructose. Controlling reaction reversibility provides an additional tool to optimize selectivity. It is interesting to note that two equivalents of LA are generated from one equivalent of sorbitol via the [3+3] route, while, only one equivalent of LA is obtained via the [2+4] route. In other words, it is advantageous to enhance the [3+3] route and depress the [2+4] route for a greater selectivity to LA.

With this mechanistic understanding in mind, we have selected several primary alcohols as additives in the model reaction under the standard reaction conditions (Figure 3b). Remarkably, the yields of LA were increased dramatically when methanol was added (Figure 3b). Full conversion and an impressive yield of 95% for LA were obtained when 5 equivalents of methanol were used. However, other alcohols have little or no influence on the selectivity (Figure 3b). These observations can be attributed to the depression the [2+4] route by adding methanol, as methanol is the product using this route according to our proposed mechanisms. More methanol was seen to decrease the activity and the selectivity, presumably because this destroyed the solute-free reaction conditions. When ethylene glycol was added, the total conversion was significantly decreased but with a complete selectivity to LA, which suggested that the addition of ethylene glycol blocks the [2+4] route and pushes the reaction equilibrium over to the [3+3] route. Figure 3b also summarizes the effects of reaction temperature. Decreasing the temperature to

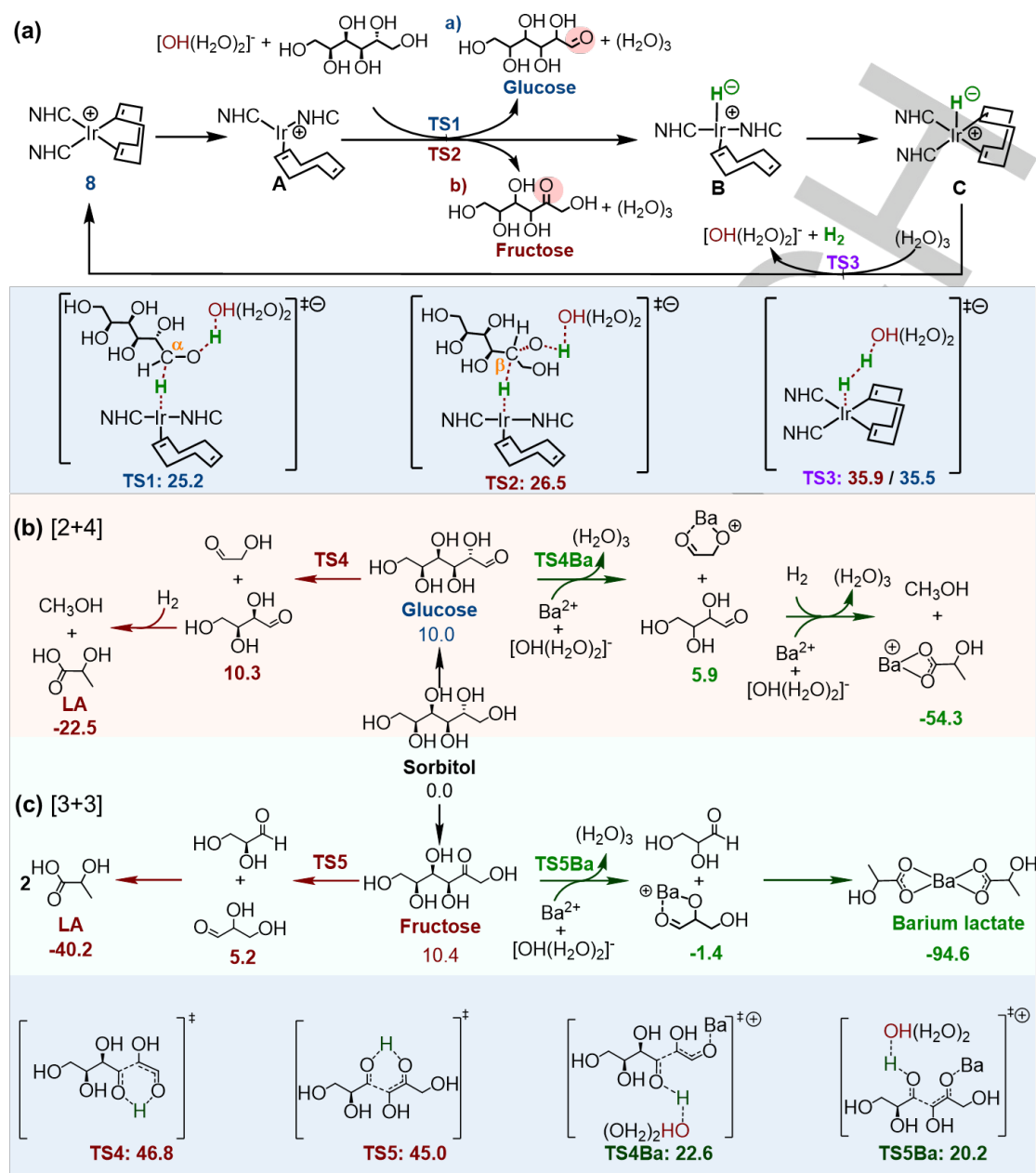


Figure 4. a) The calculated catalytic dehydrogenation from sorbitol to glucose or fructose with NHC-Ir **8** (Values are relative Gibbs free energies (ΔG , in kcal/mol) with respect to sorbitol and catalyst **8**. In addition, ΔG for the pathway to produce fructose or glucose is labeled in dark blue or dark red, respectively. Clusters of $[\text{OH}(\text{H}_2\text{O})_2]^-$ and $(\text{H}_2\text{O})_3$ are used to simulate the base and water, respectively, since these clusters represent a good compromise between accuracy and efficiency as shown^[15b,18] for the description of the proton exchange reaction. Calculated mechanisms for the generation of lactate and other by-products via b) [2+4] and c) [3+3] routes without (dark red) and with (dark green) the participation of Ba^{2+} /hydroxide.

140 °C led to a slightly higher yield (97%), while lowering the temperature led to a reduction in selectivity (88%).

Reusability of the solid catalyst. Being insoluble in water and most organic solvents, solid catalyst **5a** is well suited to recycling. Practical testing proved that this is particularly helping to build the case for an industrially viable catalytic system. After simple centrifugation, filtration, and washing with water and methanol, the solid molecular catalysts were readily recovered for the next run, when simply recharged with sorbitol, base, and

MeOH. Full conversion and almost quantitative yields of LA (>99%) were obtained in the first 11 runs under the optimized reaction conditions, demonstrating its high catalytic stability and efficiency. A slight decline of the conversion and yield was observed in the 12th run (82%) with the selectivity decreased to 89% (Figure 3c; see SI for details). When the reaction time was extended to 24 hours after these multiple runs, the conversion and yield increased slightly, while the selectivity went down slightly to 98%.

In order to understand the recycling process better, the content of iridium in the filtrate after the multiple runs was analyzed by inductively coupled plasma emission spectroscopy (ICP-AES, See Table S3). Approximately, 0.1 $\mu\text{g/mL}$ iridium leaching was observed after six runs, presumably due to a trace amount of inactive iridium species or precursors entrapped in the matrix cavities of the assemblies. The amount of leaching afterwards was negligible. The Ir content of the recovered solid **5a** after 3 runs was measured as 19.20%, which was practically the same as in the freshly prepared solid catalyst **5a** (19.82%) determined by ICP-AES and was also consistent with the theoretical value (20.02%) of $[\text{IrC}_{45}\text{H}_{44}\text{IN}_4]_n$. As investigated by SEM and TEM, the morphology of the recovered solid catalyst **5a** after 16 runs was found to be very similar to that of the newly prepared polymer (Figure S2 vs Figure S3, and Figure S11 vs S12), further confirming the stability of the solid molecular catalysts.

Encouraged by the remarkable performance of the solid molecular catalysts, a scale-up reaction using only 500 ppm **5a** was carried out. With a reaction temperature of 160 $^{\circ}\text{C}$, sorbitol was fully converted with a complete selectivity to LA in 48 hours. Reducing the catalyst loading to 150 ppm led to a large drop to only 43% conversion of sorbitol after 100 hours under the same reaction conditions, although this corresponded to an increased turn-over-number (TON) of 5700.

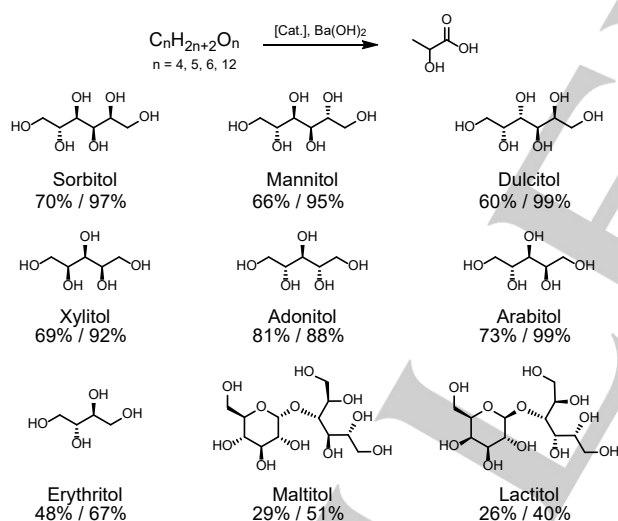


Figure 5. Substrate scope without (left values) or with (right values) the addition of 5 equiv. of methanol. Reaction conditions: sugar alcohol (3 mmol), solid catalyst **5a** (0.2 mol%), $\text{Ba}(\text{OH})_2 \cdot 8\text{H}_2\text{O}$ (2.5 equiv.), 140 $^{\circ}\text{C}$, 12 hours. Conversion and selectivity were determined by an HPLC analysis and calculated on a molar carbon basis.

Substrate scope. With a full substrate conversion and an excellent selectivity to LA in the oxidative dehydrogenation of sorbitol using only 0.2 mol % NHC-Ir solid molecular catalyst **5a**, the substrate scope of different bio-polyols containing 4, 5, 6 and 12 carbon atoms was then explored at 140 $^{\circ}\text{C}$ for 12 hours with or without the addition of 5 equiv. methanol (Figure 5). All selected

sugar alcohols, except two disaccharides, were selectively converted to LA in good to excellent yields with full conversions with or without MeOH addition. Remarkably, the addition of methanol did improve the selectivity of the oxidative dehydrogenation of sugar alcohols in all cases. Mannitol or dulcitol, as the isomer of sorbitol, gave similar yields with a full substrate conversion. These similar outcomes indicated that the different orientation of the hydroxyl groups hardly affected the dehydrogenation process. For all three kinds of bio-polyols with five carbons, a full conversion with a high selectivity to LA was achieved with the addition of methanol. However, the four carbon bio-polyol erythritol gave a poorer result possibly due to a different pathway to form LA. As the cleavage of glucosidic bonds is unlikely to happen under the alkaline condition,^[19] the yield of LA is unable to exceed 50% when using maltitol and lactitol as substrates.

Conclusion

We have made a significant advance in the production of LA from simple, low cost bio-polyols. Efficient and selective catalytic oxidative dehydrogenation was achieved using a 3D self-supported NHC-iridium catalyst described for the first time. The solid catalysts synthesized by coordination assembly showed a significantly enhanced stability with high activity and perfect selectivity for dehydrogenation of sorbitol to produce the commercially important product LA with the help of Ba^{2+} /hydroxide ions and methanol. Computational studies revealed that in the dehydrogenation of sorbitol under alkaline conditions, the ligand dissociation of the NHC-iridium catalysts was avoided via an outer-sphere catalytic pathway, which was beneficial to their structural stability. The high activity and selectivity towards LA were facilitated by the participation of Ba^{2+} /hydroxide both kinetically and thermodynamically. By blocking the [2+4] route to favor the [3+3] route, the right amount of methanol could further increase the selectivity to LA. At the optimal reaction conditions, the yield of LA has reached a remarkable 97%, which sheds light on the potential industrial production of LA from cheap and abundant biopolyols.

Acknowledgements

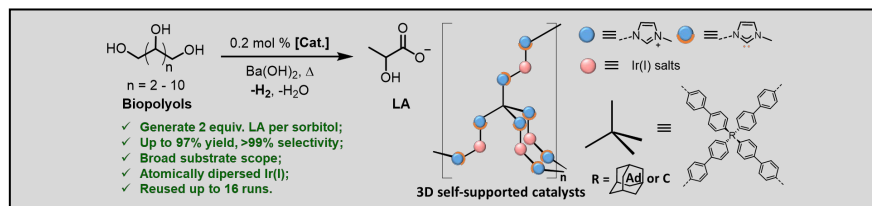
Financial supports from the National Key R&D Program of China (Nos. 2016YFA0202902 and 2018YFA0208600), the National Natural Science Foundation of China (Nos. 21861132002, 21871059, 21572036 and 21688102), and Department of Chemistry, Fudan University are gratefully acknowledged.

Keywords: Lactic acid • bio-polyols • N-heterocyclic carbene iridium complex • oxidative dehydrogenation • self-supporting

- [1] a) G. W. Huber, S. Iborra, A. Corma, *Chem. Rev.* **2006**, *106*, 4044–4098.
b) J. N. Chheda, G. W. Huber, J. A. Dumesic, *Angew. Chem. Int. Ed.*

- 2007, 46, 7164-7183; c) M. Besson, P. Gallezot, C. Pinel, *Chem. Rev.* **2014**, 114, 1827-1870; d) B. Zada, M. Chen, C. Chen, L. Yan, Q. Xu, W. Li, Y. Fu, *Sci. China Chem.* **2017**, 60, 853-869; e) S. Shylesh, A. A. Gokhale, C. R. Ho, A. T. Bell, *Acc. Chem. Res.* **2017**, 50, 2589-2597; f) T. A. Bender, J. A. Dabrowski, M. R. Gagné, *Nat. Rev. Chem.* **2018**, 2, 35-46; g) P. Sudarsanam, R. Zhong, S. Van den Bosch, S. M. Coman, V. I. Parvulescu, B. F. Sels, *Chem. Soc. Rev.* **2018**, 47, 8349-8402; h) Z. Zhang, Q. Yang, H. Chen, K. Chen, X. Lu, P. Ouyang, J. Fu, J. G. Chen, *Green Chem.* **2018**, 20, 197-205; i) H. C. Ong, W. H. Chen, A. Farooq, Y. Y. Gan, K. T. Lee, V. Ashokkumar, *Renew. Sust. Energ. Rev.* **2019**, 113, 109266; j) Y. Jing, Y. Guo, Q. Xia, X. Liu, Y. Wang, *Chem* **2019**, 5, 2520-2546.
- [2] a) L. N. Ding, A. Q. Wang, M. Y. Zheng, T. Zhang, *ChemSusChem* **2010**, 3, 818-821; b) X. Jin, B. Yin, Q. Xia, T. Fang, J. Shen, L. Kuang, C. Yang, *ChemSusChem* **2019**, 12, 71-92.
- [3] S. Esposito, B. Silvestri, V. Russo, B. Bonelli, M. Manzoli, F. A. Deorsola, M. Di Serio, *ACS Catal.* **2019**, 9, 3426-3436.
- [4] a) Y. Jia, H. Liu, *Chin. J. Catal.* **2015**, 36, 1552-1559; b) X. Guo, J. Guan, B. Li, X. Wang, X. Mu, H. Liu, *Sci. Rep.* **2015**, 5, 1-9.
- [5] M. G. Manas, J. Campos, L. S. Sharninghausen, E. Lin, R. H. Crabtree, *Green Chem.* **2015**, 17, 594-600.
- [6] M. Dusselier, P. Van Wouwe, A. Dewaele, E. Makshina, B. F. Sels, *Energ. Environ. Sci.* **2013**, 6, 1415-1442.
- [7] M. Iglesias, L. A. Oro, *Chem. Soc. Rev.* **2018**, 47, 2772-2808.
- [8] a) L. S. Sharninghausen, J. Campos, M. G. Manas, R. H. Crabtree, *Nat. Commun.* **2014**, 5, 5084; b) J. Campos, L. S. Sharninghausen, R. H. Crabtree, D. Balcells, *Angew. Chem. Int. Ed.* **2014**, 53, 12808-12811; *Angew. Chem.* **2014**, 126, 13022-13025; c) L. S. Sharninghausen, R. H. Crabtree, *Isr. J. Chem.* **2017**, 57, 937-944.
- [9] P. Nikolaidis, A. Poulikkas, *Renew. Sust. Energ. Rev.* **2017**, 67, 597-611.
- [10] a) L. X. Dai, *Angew. Chem. Int. Ed.* **2005**, 43, 5726-5729; *Angew. Chem.* **2005**, 116, 5846-5850; b) Z. Wang, G. Chen, K. Ding, *Chem. Rev.* **2009**, 109, 322-359.
- [11] a) Z. Sun, Y. Liu, J. Chen, C. Huang, T. Tu, *ACS Catal.* **2015**, 5, 6573-6578; b) J. Chen, J. Wu, T. Tu, *ACS Sustain. Chem. Eng.* **2017**, 5, 11744-11751; c) Z. Sun, J. Chen, T. Tu, *Green Chem.* **2017**, 19, 789-794; d) Y. Zhang, J. Wang, H. Zhu, T. Tu, *Chem. Asian J.* **2018**, 13, 3018-3021.
- [12] W. She, K. Luo, C. Zhang, G. Wang, Y. Geng, L. Li, B. He, Z. Gu, *Biomaterials* **2013**, 34, 1613-1623.
- [13] a) Q.-H. Fan, K. Ding, Enantioselective catalysis with structurally tunable immobilized catalysts. In *Asymmetric Catalysis from a Chinese Perspective* (pp. 207-245). Springer, Berlin, Heidelberg **2011**; b) R. Zhong, A. C. Lindhorst, F. J. Groche, F. E. Kühn, *Chem. Rev.* **2017**, 117, 1970-2058.
- [14] a) O. Blum, D. Milstein, *J. Am. Chem. Soc.* **2002**, 124, 11456-11467; b) A. Azua, J. A. Mata, E. Peris, *Organometallics* **2011**, 30, 5532-5536; c) W. Kuriyama, T. Matsumoto, O. Ogata, Y. Ino, K. Aoki, S. Tanaka, T. Saito, *Org. Process Res. Dev.* **2012**, 16, 166-171; d) J. J. A. Celaje, Z. Lu, E. A. Kedzie, N. J. Terrile, J. N. Lo, T. J. Williams, *Nat. Commun.* **2016**, 7, 11308; e) S. Movassaghi, S. Singh, A. Mansur, K. K. Tong, M. Hanif, H. U. Holtkamp, C. G. Hartinger, *Organometallics*, **2018**, 37, 1575-1584.
- [15] a) B. Fang, J. H. Kim, M. S. Kim, J. S. Yu, *Acc. Chem. Res.* **2013**, 46, 1397-1406; b) Y. Shen, Q. Zheng, H. Zhu, T. Tu, *Adv. Mater.* **2020**, 32, 1905950.
- [16] I. Y. Zhang, X. Xu, Y. Jung, W. A. Ill. Goddard, *Proc. Natl. Acad. Sci. U. S. A.* **2011**, 108, 19896-19900.
- [17] Y. Wang, W. Deng, B. Wang, Q. Zhang, X. Wan, Z. Tang, H. Wan, *Nat. Commun.* **2013**, 4, 2141.
- [18] J. Joubert, F. Delbecq, *Organometallics* **2006**, 25, 854-861.
- [19] a) W. Deng, Q. Zhang, Y. Wang, *Catal. Today* **2014**, 234, 31-41; b) Y. Dai, C. Shao, Y. Piao, H. Hu, K. Lu, T. Zhang, S. Man, *Carbohydr. Polym.* **2017**, 178, 34-40.

Entry for the Table of Contents



Bio-polyols conversion: A series of 3D porous self-supported NHC-iridium coordination polymers were prepared and could function as recyclable solid molecular catalysts for dehydrogenation of bio-polyols to lactic acid with excellent activity and selectivity due to the synergistic participation of the Ba²⁺ and hydroxide ions, as well as the blockage of unwanted pathways by adding methanol.